Catal Lett (2012) 142:1141–1149
DOI 10.1007/s10562-012-0879-0

Effect of SiO_2–Al_2O_3 Composition on the Catalytic Performance of the Re_2O_7/SiO_2–Al_2O_3 Catalysts in the Metathesis of Ethylene and 2-Pentene for Propylene Production

Weena Phongsawat · Benjamas Netiworaruksa · Kongkiat Suriye · Piyasan Praserthdam · Joongjai Panpranot

Received: 21 May 2012 / Accepted: 15 July 2012 / Published online: 2 August 2012

Abstract The production of propylene via a gas-phase metathesis of ethylene and 2-pentene has been studied over the Re_2O_7/SiO_2–$x$$Al_2O$ catalysts containing various SiO_2–Al_2O_3 compositions (13, 25, 50, 75, and 100 wt% Al_2O_3). Using ethylene and 2-pentene as the reactants, isomerization of the initial 1-butene product into 2-butenes and a subsequent secondary metathesis reaction between 2-butenes and excess ethylene enhanced the propylene formation so that propylene yield higher than its stoichiometric amount (>50 %) could be obtained. While the pure Al_2O_3 supported Re_2O_7 catalyst possessed only the first type of isolated monomeric ReO_4^- tetrahedra structure with a stronger Re–O-support bond, the second type with a weaker Re–O-support bond was observed on the SiO_2–Al_2O_3 supported ones. The double-bond isomerization and the metathesis activities were optimized to produce the highest propylene yield over the Re_2O_7/SiO_2–Al_2O_3 catalyst containing 50 wt% Al_2O_3.

Keywords Metathesis · Isomerization · Propylene production · 2-pentene · Silica–alumina

1 Introduction

Olefin metathesis is one of industrial important reactions in olefin conversion that opens up many new routes to produce important petrochemical products. Current commercial technology for producing propylene via metathesis reaction is based on the conversion of ethylene and 2-butene over heterogeneous catalyst systems [1–4]. However, this route has some drawbacks although high propylene yield can be obtained. It needs C_4 streams that are free of isobutene and butadiene [5] and both cost and demand of butene industrial feedstock have increased continuously [4, 6, 7]. In our recent work, a cross-metathesis of ethylene and 2-pentene over Re_2O_7/Al_2O_3 catalysts has been studied as an interesting route to produce propylene from cheaper raw materials [8, 9]. The products from this route are not only high valuable propylene but also 1-butene that are increasing in both demand and cost nowadays [6, 7].

The Re_2O_7/Al_2O_3 catalysts have been employed in large scale metathesis of ethylene and 2-butene into propylene [10]. Their catalytic activities can be further improved by the use of mixed metal oxides supports such as SiO_2–Al_2O_3 [2, 11–13], phosphated alumina (AIPO) [14] and Al_2O_3–B_2O_3 [15]. In addition, recently mesoporous materials have been studied as supports for Re_2O_7 catalysts in the metathesis reactions [16–22]. The improved catalytic activity of the mesoporous alumina supported Re_2O_7 than those supported on conventional alumina was directly correlated to their large pore size and higher specific surface area [16]. However, the synthesis of these mesostructured oxides was more complicated and may not be suitable for industrial application [23].

W. Phongsawat · B. Netiworaruksa · P. Praserthdam · J. Panpranot (✉)
Department of Chemical Engineering, Faculty of Engineering, Center of Excellence on Catalysis and Catalytic Reaction Engineering, Chulalongkorn University, Bangkok 10330, Thailand
e-mail: joongjai.p@chula.ac.th

K. Suriye
SCG Chemicals Co., Ltd, 1 Siam-cement Rd Bang sue, Bangkok 10800, Thailand

Among the various mixed oxides used to stabilize the Re species in the favorable oxidation state for the formation of the rhenium carbene active complex, the SiO_2–Al_2O_3 receives considerable attention and has shown significant improvement in the metathesis reaction. According to the literature [2, 24, 25], low rhenium-loading Re_2O_7/Al_2O_3 catalysts exhibited poor or negligible activity for the alkene metathesis. However, 2 wt% Re_2O_7 over SiO_2–Al_2O_3 was found to be more active than the 18 wt% Re_2O_7/Al_2O_3 catalysts [26, 27]. In epoxidation of alkenes, the stability of rhenium-based catalysts also depended on the alumina content of mixed silica–alumina supports in which ReO_4^- supported on higher alumina content or pure alumina supports showed no metal lost [28] According to Moulijn and Mol [12], the Si–O–Re bonds are very weak comparing to the Al–O–Re bonds.

Acidity of the catalysts plays an important role in alkene metathesis reactions [1, 2, 13, 26, 27, 29, 30]. In general, silica–alumina is more acidic than alumina [31] and it contains both strong Lewis and Brönsted acidic sites [13, 30]. Xiaoding et al. [13, 27] showed the distinct correlation between the Brönsted acidity which was directly proportional to the silica–alumina compositions and the metathesis activity for the Re-based catalyst. A model for the generation of metallacarbenes including the function of partial reduced rhenium species and neighboring Brönsted acid sites has been proposed [27, 32]. The presence of Al in the SiO_2–Al_2O_3 supports was found to affect the performance of MoO_3/SiO_2–Al_2O_3 catalysts in various works [33–39]. Debecker et al. [33] suggested that the acidity created by the presence of alumina in silica was beneficial for the better dispersion of active Mo species.

A number of previous studies of Re-based catalysts [27, 28, 30, 40–43] have shown that double-bond isomerization activity of silica–alumina was much higher than that of alumina. The isomerization activity of Re_2O_7/SiO_2–Al_2O_3 catalyst was even more higher than the corresponding sole SiO_2–Al_2O_3 support [40]. Nevertheless, in our previous studies [8, 9], double-bond isomerization of 1-butene was found to be useful for producing additional propylene formation in the unconventional metathesis of ethylene and 2-pentene. The present work was aimed to further investigate the influence of SiO_2–Al_2O_3 composition on the catalytic performances of Re_2O_7/SiO_2–Al_2O_3 in the metathesis of ethylene and 2-pentene for propylene production. The catalysts were also characterized by inductively coupled plasma optical emission spectroscopy (ICP-OES), N_2-physisorption (BET and BJH methods), X-ray diffraction (XRD), temperature program desorption of NH_3 (NH_3-TPD), X-ray photoelectron spectroscopy (XPS), UV–Visible, and FT-Raman spectroscopy.

2 Experimental

2.1 Catalyst Preparation

2.1.1 *Synthesis of SiO_2–Al_2O_3 Supports*

The SiO_2–$x Al_2O_3$ supports containing various amount of alumina (x = 13, 25, 50, 75, and 100 wt%) were prepared by a co-precipitation method according to that of Okada et al. [44]. Aluminium nitrate nonahydrate [ANN; $Al(NO_3)_3 \cdot 9H_2O$] and tetraethylorthosilicate [TEOS; $Si(OC_2H_5)_4$] solution were coprecipitated and adjusted to 1.2 mol l^{-1} for all the sample preparation. The distilled water and ethanol was first mixed, then ANN was added and the resulting solution was stirred for 15 min. The amount of H_2O in the solution was adjusted to give H_2O/TEOS = 18/1, this ratio indicating a large excess of H_2O for hydrolysis of TEOS. An ethanol solution containing a desired amount of TEOS was then added and stirred for 3 h, 25 wt% of ammonia solution was added rapidly to the solution with vigorous stirring. The precipitates were immediately dried over a hot plate at 60 °C for 3 h and subsequently dried overnight at 110 °C in an oven. After drying, they were calcined under oxygen flowing at 300 °C for 4 h with a heating rate of 3 °C/min to obtain the xerogels. These xerogels were then calcined at 550 °C for 4 h under oxygen flowing with a heating rate of 10 °C min^{-1} before used as the SiO_2–Al_2O_3 supports for preparation of supported rhenium oxide catalysts. The synthesized SiO_2–Al_2O_3 supports were denoted as Si*x*Al where x indicated wt% of Al_2O_3 in the silica–alumina supports.

2.1.2 *Preparation of Supported Rhenium Oxide Catalysts*

The catalysts were prepared by incipient wetness impregnation with aqueous solution of ammonium perrhenate (99.999 %, Aldrich). When quantity of the solution of the desired Re-metal loading (8 wt% Re-metal) was greater than pore volume of the supports, the impregnation was performed several times with drying at 110 °C in between to eliminate the solvent for 6 h. After impregnation, these catalysts were dried overnight at 110 °C and then calcined at 550 °C for 8 h under oxygen flow with a heating rate of 10 °C min^{-1}. The catalyst nomenclature Re/Si*x*Al is referred to the Re_2O_7 supported on the SiO_2–$x Al_2O_3$ containing x wt% of Al_2O_3.

2.2 Catalyst Characterization

The weight percentage of actual Re metal for each catalyst after calcination was measured by ICP-OES on a Perkin Elmer Optima 2100DV. The samples were digested with hydrofluoric and nitric acid at 60 °C. The specific surface area, pore volume, average pore diameter and pore sizes distribution of the supports and the supported rhenium catalysts were measured by the N_2-physisorption with using a Micrometritics model ASAP 2000 automated system. The measurements were performed with a degassing at 350 °C (Ramp rate $= 10$ °C min^{-1}) for 4 h prior to N_2 physisorptions at -196 °C. The specific surface area was calculated based on the Brunauer–Emmett–Teller (BET) isotherms and the pore volume and pore size distribution were calculated based on the Barrett–Joyner–Halenda (BJH) desorption branch analysis. The XRD patterns of the supports and the catalysts were measured in a range of 2θ value between 20° and 80° at a rate of 0.02° s^{-1} using a SIEMENS D5000 X-ray diffractometer and Cu K_α radiation with a Ni filter. The PCPDFWIN database was used as reference to identify the crystalline phases. The NH_3-TPD measurements were carried out in a quartz U-tube reactor using a Micromeritic Chemisorb 2750 automated system. The catalyst samples were firstly pretreated in a He flow (25 ml min^{-1}) at 200 °C for 2 h prior to measurement. Subsequently they were cooled to room temperature around 25 °C then a 30 %NH_3/He mixed gas was flowed (25 ml min^{-1}) over the samples for 1 h to throughout adsorb on the acid sites. After ammonia adsorption on catalyst surface was completed, the excess ammonia was eradicated by the He flowing (25 ml min^{-1}) at the room temperature for 1 h. Then, the samples were heated linearly with a rate of 10 °C min^{-1}. The TPD profiles were detected by TCD detector and analyzed with a ChemiSoft TPx software. XPS was carried out using an AMICUS photoelectron spectrometer equipped with an Mg K_α X-ray as a primary excitation and KRATOS VISION2 software. XPS elemental spectra were acquired with 0.1 eV energy step at a pass energy of 75 eV. All the binding energies were referenced to the C 1 s peak at 285 eV. Diffuse reflectance UV–Vis spectra were collected on Lambda 650 UV–Vis spectrometer equipped with a diffuse reflectance attachment and an integrating sphere. The samples were studied in the form of powder carried out in sample holder. The spectra were recorded under air-exposed conditions in the range 200–900 nm and the scan speed was 1 nm min^{-1}.

2.3 Catalytic Tests

The catalytic performances were tested in the gas-phase metathesis reaction between ethylene and 2-pentene, which was carried out in a stainless steel ($ID_{tube} = 0.7$ cm) fixed-bed tabular flow reactor under atmospheric pressure. The gas-phase of 2-pentene was prepared by dilution a small amount liquid 2-pentene (≥ 99 % mixture of isomers, Aldrich) in low pressure N_2 gas (4 vol.% of 2-pentene in 12 bar N_2 balance). The reactants were pre-mixed with high purity ethylene (99.999 %), and high purity N_2 to have the composition of 6.75 vol.% 2-pentene, 2.25 vol.% ethylene in N_2 balance before passing through the reactor. The feed flow rates were adjusted to 70–77.5 cm^3 min^{-1} depending on the bed volume of each catalyst. In a typical run, 1 g of the catalyst sample was placed in the middle of the reactor. The reaction temperature, gas hourly space velocity (GHSV), and mole of feed ratio (ethylene/2-pentene) were kept at 35 ± 2 °C, 3,000 h^{-1} and 3, respectively. Start up with pretreatment the catalyst sample at 500 °C under N_2 flow for 1 h and then cooled down to the reaction temperature. The analysis of reaction products was started after an initial reaction for 35 min. Both reactants and products of reaction were followed and analyzed every half an hour using an on-line gas chromatograph (Agilent GC 7820A) equipped with a capillary GS-Gaspro113-4362 column (60 m × 0.32 mm). The GC signals were collected using an EZChrom Elite integrated peak program integrator.

3 Results and Discussion

3.1 Catalytic Performances of the Re/Si*x*Al Catalysts

The catalytic performances of the SiO_2–xAl_2O_3 supported rhenium oxide catalysts were evaluated in the gas-phase metathesis reaction of ethylene and 2-pentene at 35 °C, GHSV 3,000 h^{-1}, and ethylene/2-pentene mole ratio = 3. The conversion of 2-pentene, the yield of propylene, 1-butene, and 2-butene as a function of time-on-stream are shown in Fig. 1a–d, respectively. The conversion of 2-pentene in average at 485 min time-on-stream was ranging between 97 and 84 %. However, lower 2-pentene conversion was obtained over the Re/Si13Al and Re/Si25Al whereas those supported on the SiO_2–xAl_2O_3 containing higher amounts of Al_2O_3 Re/Si50Al, Re/Si75Al, and Re/100Al exhibited higher 2-pentene conversion at ca. 95–97 %. As shown in Eq. (1), the theoretical stoichiometric value of reactants in the metathesis reaction of ethylene and 2-pentene is equimolar.

$$CH_2 = CH_2 + CH_3CH = CHCH_2CH_3 \leftrightarrow CH_2 = CH_2CH_3 + CH_2 = CHCH_2CH_3 \tag{1}$$

The conversion of limited 2-pentene reactant and the yield of products were calculated using the following equations:

$$\text{Conversion of 2-pentene } (\%) = 100 \times \frac{\text{amount of 2-pentene in feed} - \text{amount of 2-pentene remained in products}}{\text{amount of 2-pentene in feed}}$$

$$\text{Yield of component i } (\%) = \text{conversion of 2-pentene} \times \frac{\text{amount of component i in products}}{\text{amount of total products}}$$

In the present work, the propylene yields for all the Re/SixAl catalysts far exceeded the stoichiometric values (propylene selectivity of 50 mol% or ~ 43 wt%). Only the Re/100Al exhibited propylene yield equal to the stoichiometric value. The highest propylene yield ca. 70 % was achieved over the Re/Si50Al with good stability during the 488 min time-on-stream. Thermodynamically, excess ethylene would shift the reaction (1) from left to right, producing more propylene and 1-butene products. However, as shown in Fig. 1, the yield of 1-butene product was not increased in the same trend as that of propylene for the catalysts exhibiting propylene yield higher than its stoichiometric amount (i.e., for Re/Si50Al and Re/Si75Al). It has been suggested that the isomerization of 1-butene product from the metathesis of ethylene and 2-pentene to 2-butenes (Eq. 2) can further react with excess ethylene in the feed, resulting in additional propylene formation (Eq. 3) [8, 9].

$$\text{Isomerization}: \quad CH_2 = CHCH_2CH_3 \rightarrow CH_3CH_2 = CH_2CH_3 \tag{2}$$

$$\text{Secondary metathesis}: \quad CH_2 = CH_2 + CH_3CH_2 = CH_2CH_3 \rightarrow 2(CH_2 = CH_2CH_3) \tag{3}$$

The yield of 1-butene was found to be varied from 55 % for the Re/100Al, 30 % for the Re/Si75Al, and <20 % for the other catalysts (Re/Si13Al, Re/Si25Al, and Re/Si50Al). The lowest yield of 1-butene was obtained over the

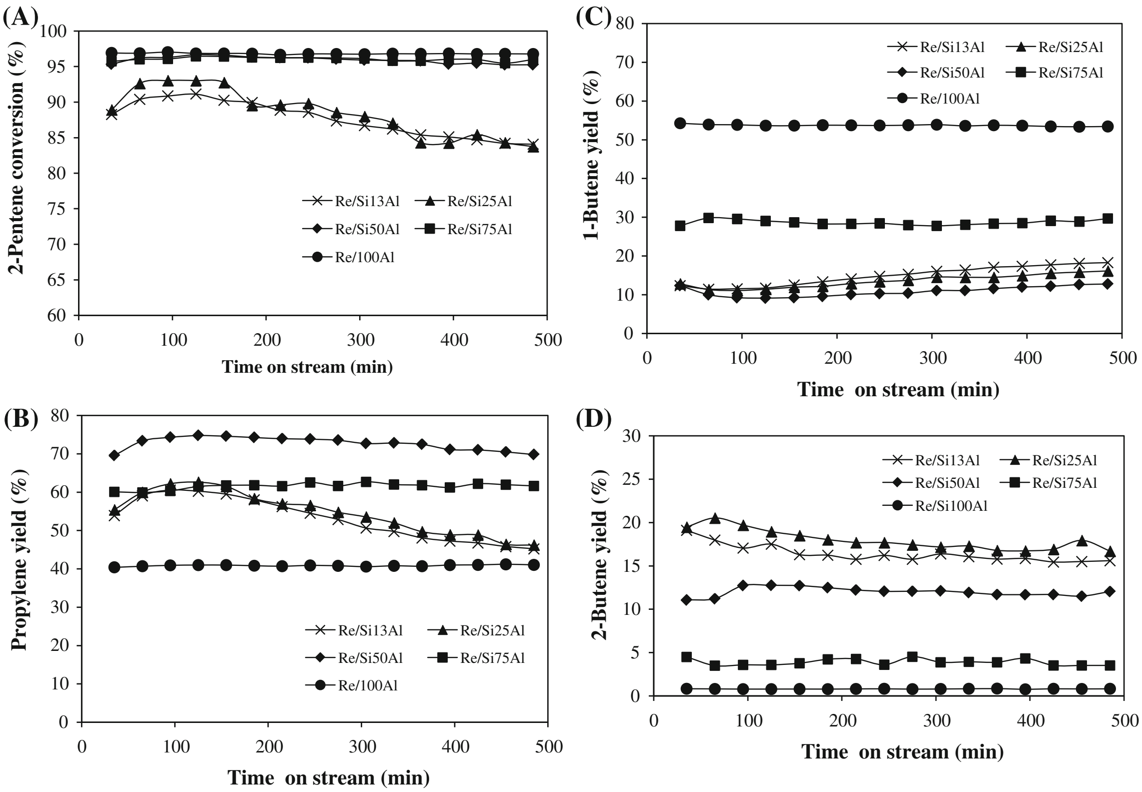

Fig. 1 Effect of silica–alumina composition (SiO_2–xAl_2O_3, $x = 13$, 25, 50, 75 and 100 wt% Al_2O_3) of Re_2O_7/SiO_2–xAl_2O_3 catalysts on the **a** 2-pentene conversion, **b** propylene yield, **c** 1-butene yield, **d** 2-butene yield. (Pressure: 0.1 MPa; E/2P mole ratio: 3; GHSV: 3,000 h^{-1}; Temperature: 35 °C)

Re/Si50Al, suggesting that 1-butene was isomerized to 2-butene and further reacted with excess ethylene to form additional propylene product. This view point can also be considered in terms of the yield of 2-butene, higher yields of 2-butene were produced over the Re_2O_7 catalysts supported on the relatively high silica content supports (Re/Si13Al and Re/Si25Al) whereas moderately high and lower 2-butene yields were obtained over Re/Si50Al and Re/75–100Al catalysts, respectively. Both the isomerization and the cross-metathesis activity strongly depended on the Si/Al composition of the SiO_2–$x$$Al_2O_3$ supports. Unlike the conventional metathesis of ethylene and 2-butenes that double-bond isomerization was a competing side reaction; it was considered as a useful reaction for the transformation of 1-butene primary product to 2-butenes which could further react with excess ethylene to form additional propylene in the metathesis of ethylene and 2-pentene [8, 9]. The results in this study, however, suggest an optimum composition of the SiO_2–Al_2O_3 supports for the Re_2O_7 catalysts to exhibit high activities for both double-bond isomerization and cross-metathesis reactions so that higher propylene yield (than its stoichiometric amount) was attained with high stability. Besides propylene and 1-butene primary metathesis products, the other by-products including *cis*- and *trans*-2-butene, 1-pentene, 3-hexene, and C_{5+} oligomers can also be produced by various side reactions [8]. However, under the reaction conditions used in the present study, the only C_{5+} hydrocarbon found in the products was 3-hexene, which was produced in very small amount (<3 % yield) by self-metathesis of 2-pentene. A relationship between the catalyst physicochemical properties and their catalytic performances was further investigated by catalyst characterization using several techniques.

3.2 Catalyst Characterization

The BET surface area, pore volume, and average pore diameter of the supports and the supported rhenium oxide catalysts are shown in Table 1. It was found that all the SiO_2–$x$$Al_2O_3$ supports had larger BET surface area and pore volume than that of the pure Al_2O_3 which is in good agreement with those of Okada et al. [44]. However, considering the changes in BET surface area, pore volume, and pore diameter of the supports after impregnation of rhenium metal and calcination, the Re/Si50Al exhibited the least change in their textural properties. Such results suggest that most of the rhenium was highly dispersed on the surface of the SiO_2–$x$$Al_2O_3$ support. As revealed by ICP-OES results, the actual Re-metal loadings varied from 4.6 to 8.1 wt%, depending on the supports used. Higher amount of Re-metal (7.8–8.1 wt%) remained on the Al_2O_3 rich supports (≥50 wt% Al_2O_3). Because some of the Re_2O_7 can be volatized during high temperature calcination step especially the inactive rhenium centers of the type $\equiv$Si–O–ReO_3 [40], the use of SiO_2–$x$$Al_2O_3$ supports with relatively higher silica content (i.e., Si13Al and Si25Al) resulted in lower amount of rhenium metal on the catalyst samples. It is quite well known that Re_2O_7/SiO_2 catalyst has no activity in olefin metathesis due to poor interaction between silica and rhenium oxide that tends to form inactive rhenium clusters [45].

Although one can notice the differences in the actual Re metal loadings on the various Re_2O_7/SiO_2–$x$$Al_2O_3$ catalysts, they seemed to make little influence on the catalytic performances. The amount of 2-pentene converted per gram Re metal was calculated and was found to be even higher on the catalysts with lower Re contents (Re/Si13Al and Re/Si25Al). However, it is quite well known that the number of rhenium active sites were only small fraction of

Table 1 The physicochemical property of the bare silica-alumina supports and the supported rhenium oxide catalysts

Sample	Al_2O_3 content[a] (wt%)	Surface area[b] (m^2 g^{-1})	Pore volume[c] (cm^2 g^{-1})	Average pore diameter[c] (nm)	Re-metal loading[d] (wt%)	Total acidity[e] (10^3 µmol NH_3 g^{-1})
Re/Si13Al	13	224 (291)	1.10 (1.07)	13.7 (17.2)	4.7	7.487
Re/Si25Al	25	210 (277)	0.71 (0.58)	8.7 (9.7)	4.6	7.333
Re/Si50Al	50	308 (316)	0.83 (0.79)	8.3 (8.7)	7.5	14.554
Re/Si75Al	75	389 (431)	0.86 (0.77)	6.1 (6.0)	7.8	14.967
Re/100Al	100	213 (233)	0.40 (0.33)	5.1 (4.9)	8.2	7.698

The numbers in parenthesis indicated the values of the bare supports

[a] Based on the calculated amounts that were used for synthesis of various SiO_2–Al_2O_3 supports

[b] Based on the Brunauer–Emmett–Teller (BET) method

[c] Based on the Barret–Joyner–Halenda (BJH) desorption method

[d] Actual re-metal loading for each catalyst after calcination was measured by ICP-OES

[e] Total surface acidity of the catalysts was probed by the NH_3-TPD

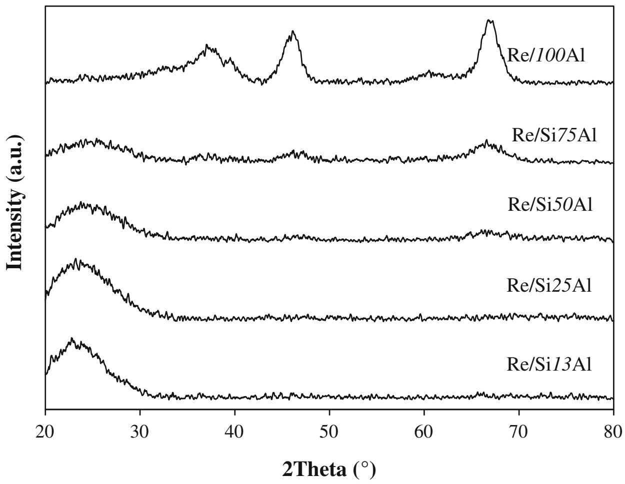

Fig. 2 The X-ray diffraction (XRD) patterns of the different Re_2O_7/SiO_2–xAl_2O_3 catalysts ($x = 13$, 25, 50, 75 and 100 wt% Al_2O_3)

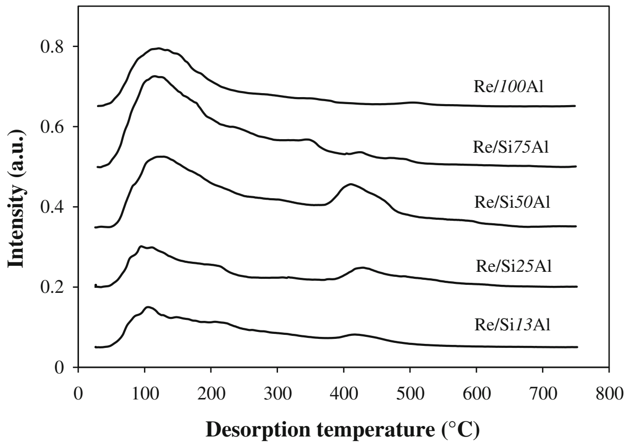

Fig. 3 Temperature programmed desorption of ammonium (NH_3-TPD) spectra of the Re_2O_7/SiO_2–xAl_2O_3 catalysts ($x = 13$, 25, 50, 75 and 100 wt% Al_2O_3)

the Re atoms presented on supported rhenium oxide catalysts. The rhenium active centers have been quantitatively determined by various techniques including poisoning experiments using NO [4], kinetic studies [46], and chemical counting method [47]. These studies showed the percentage of active Re centers of approximately 1 % of the total actual amount Re loading.

The XRD patterns of the Re/Si*x*Al catalysts are shown in Fig. 2. A broad peak around 20–30° represents a typical character of amorphous solid of these samples. The XRD characteristic peaks of the γ-phase alumina appeared at $2\theta = 32$, 37, 46, 61 and 67° for the samples containing $\geq$50 wt% of Al_2O_3. The intensity of the γ-phase alumina increased with increasing amount of Al_2O_3 in the samples. The peaks corresponding to the crystalline Re_2O_7 were not detected for all the supported Re_2O_7 catalysts. According to the literature [2, 16, 42, 48], most of the rhenium species formed on the surface is isolated ReO_4^- form and the crystalline Re_2O_7 can be volatilized during high temperature calcination at above 300 °C.

Although alkene metathesis reaction does not regard as an acid-catalyzed reaction, surface acidity of the catalysts strongly influences the formation of metathesis active sites [2, 26, 27, 29, 33, 49]. Acidity of the catalysts was probed by the NH_3-TPD measurements and the results are shown in Fig. 3. The total amounts of acidity was found to be directly related to the specific surface area of the catalysts, in which they were increased with increasing alumina content from 13 to 75 wt% and then markedly declined for the 100 wt% Al_2O_3 support (Table 1). It is generally accepted that silica–alumina supported metathesis catalysts are more acidic than alumina supported catalysts [2, 11–13]. From the NH_3-TPD profiles (Fig. 3), the desorption peaks in the temperature range below and above 300 °C were assigned to the weak and the strong acid sites, respectively [8, 9]. In Fig. 4, it was found that the amount of strong acid sites was maximized for the Re/Si50Al. The Re/100Al_2O_3 shows only the weak acidity characteristic. The acid strength thus strongly influenced both the isomerization and metathesis activity over the supported Re_2O_7 catalyst. Since the major products of the metathesis of ethylene and 2-pentene obtained over the Re/*100*Al_2O_3 catalyst were in accordance with their stoichiometric amounts, it is suggested that the weak acidity of the Re/100Al_2O_3 was not strong enough for isomerization reaction of the 1-butene product so that the secondary metathesis reaction did not occur.

The oxidation states of rhenium in the various Re_2O_7/SiO_2–Al_2O_3 catalysts were determined by XPS and the results are shown in Fig. 5. According to the literatures [50–52], the XPS spectra revealed that most of rhenium oxidation state of the fresh catalysts lied in oxidation state

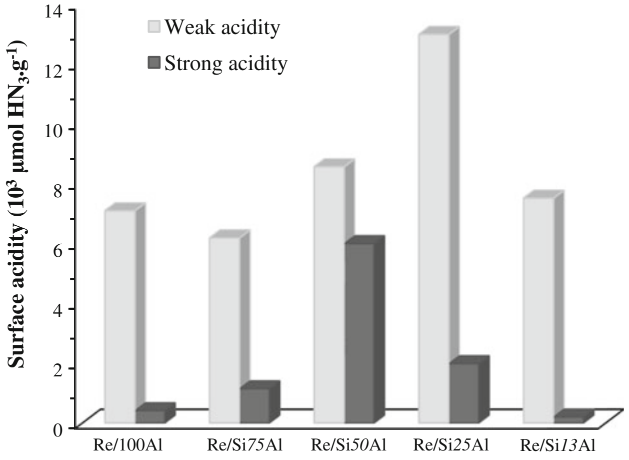

Fig. 4 The amount of surface acidity of the different Re_2O_7/SiO_2–xAl_2O_3 catalysts in terms of µmol NH_3 per gram of catalysts by classification into weak and strong acidity

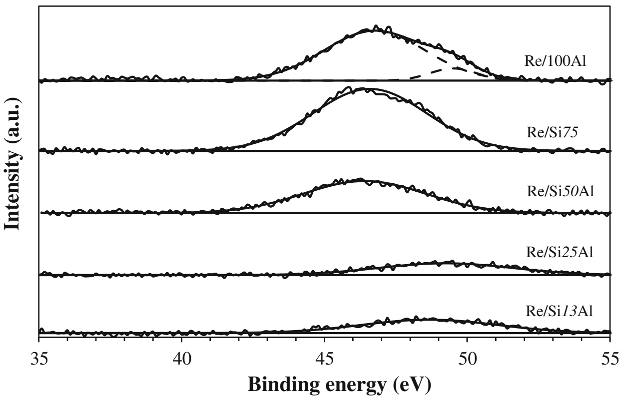

Fig. 5 XPS spectra of the fresh Re_2O_7/SiO_2–xAl_2O_3 catalysts ($x = 13$, 25, 50, 75 and 100 wt% Al_2O_3)

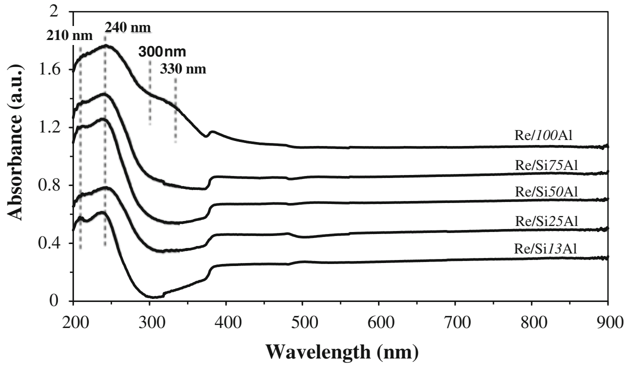

Fig. 6 Diffuse reflectance UV–Visible spectra of the different Re_2O_7/SiO_2–xAl_2O_3 catalysts ($x = 13$, 25, 50, 75 and 100 wt% Al_2O_3)

+(7), however a fraction of rhenium oxidation state +(6–7) was also detected for the Re_2O_7/SiO_2–$50Al_2O_3$, Re_2O_7/SiO_2–$75Al_2O_3$ and $Re_2O_7/100Al_2O_3$ catalysts. Based on the XPS results, the catalysts in this study can be categorized into three different characters; the first one is the group of low metal–support interaction Re_2O_7/SiO_2–$13Al_2O_3$ and Re_2O_7/SiO_2–$25Al_2O_3$ catalysts possessing only the rhenium oxidation state +(7). The second one is the group of stronger metal–support interaction Re_2O_7/SiO_2–$50Al_2O_3$ and Re_2O_7/SiO_2–$75Al_2O_3$ catalysts that showed lower binding energy of the rhenium oxidation state +(6–7). Both of the rhenium species (Re^{7+} and Re^{6-7+}) were detected on the surface of the $Re_2O_7/100Al_2O_3$ catalysts, the third type possessing metal–support interaction strength in between the first two groups. The different characteristics observed may be related to the dispersion degree of rhenium oxide on the surface. Well-dispersion species were found on the SiO_2–$50Al_2O_3$ and the SiO_2–$75Al_2O_3$. Iwasawa and Yuan [52] also found that the binding energy of rhenium species shifted towards lower binding energy for the catalysts possessing stronger metal–support interaction.

The structure of transition metal species was investigated by diffuse reflectance UV–Visible spectroscopy. The diffuse reflectance UV–Visible spectra of the various supported Re_2O_7 catalysts are shown in Fig. 6. Two intense absorption bands centered at ca. 210 and 240 nm were assigned to the undistorted tetrahedral ReO_4^- ion [53]. The presence of isolated tetrahedral species of rhenium active species was found on the Re_2O_7/SiO_2–xAl_2O_3 composing of higher alumina content ($x \geq 50$ wt% Al_2O_3). Hence, it would be an evidence for the highly dispersion of rhenium over these suitable support compositions. The isolated tetrahedral structure of rhenium is necessary for the formation of metal–carbene metathesis active sites and better catalyst performance. The $Re/100Al_2O_3$ shows additional absorption bands centered at ca. 300 and 330 nm which were attributed to the existence of rhenium in a distorted octahedral species [13, 53].

The surface structures of ReO_x species on the various supported Re_2O_7 catalysts were characterized by Raman spectroscopy and the results are shown in Fig. 7. Consistent to the XRD results, the Raman shifts corresponding to the crystalline Re_2O_7 (at 800, 450, and below 200 cm^{-1}) [54, 55] were not detected for all the catalyst samples and only isolated ReO_4^- species existed. The monomeric tetrahedral ReO_4^- ions were observed at $\sim$990–975 cm^{-1} [ν_s(Re=O), the most intense band], $\sim$900–930 cm^{-1} [ν_{as}(Re=O), weak band], and $\sim$340 cm^{-1} [$\delta_{s,\,as}$(O–Re–O), intense band] [48, 54–57]. For all the SiO_2–xAl_2O_3 supported Re_2O_7 catalysts, two separated peaks of the terminal Re=O bond were observed at 970 and 990 cm^{-1}, indicating the existence of two different surface rhenium oxide species. The position of the higher frequency peaks tended to shift to lower frequency when the alumina composition in the SiO_2–xAl_2O_3 supports increased and eventually merged into a single peak at 976 cm^{-1} for the case of Re/100Al catalyst. The shift of Raman to lower frequency was interpreted as a result of the stronger of the bridging Re–O-support bond strength [58, 59]. The $Re/100Al_2O_3$

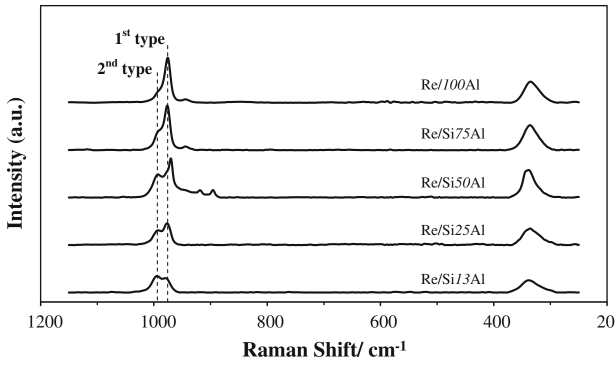

Fig. 7 Raman spectra of the different Re_2O_7/SiO_2–xAl_2O_3 catalysts ($x = 13$, 25, 50, 75 and 100 wt% Al_2O_3)

catalyst showed metathesis activity with negligible isomerization activity. It is likely that the catalyst had only one type of surface rhenium species with rather strong Re–O-support bond (shown as a single Raman shift at 976 cm^{-1}). Contrarily, all the Re/Si*x*Al catalysts exhibited double-bond isomerization activity in addition to the metathesis reaction. The second type of surface rhenium species with a weaker Re–O-support bond (additional peak at 990 cm^{-1}) could be attributed to the hydrido–rhenium species ([Re]–H) which was claimed to act as isomerization sites [30, 42, 60]. The Raman spectroscopy results strongly support the UV–Vis results that isolated monomeric ReO_4^- tetrahedra is the rhenium metathesis active structure. It is noted that the hydrolyzed ReO_4^- or the ReO_4^- ion in aqueous solution also resemble in the form of isolated monomeric ReO_4^- tetrahedral species [54, 57, 61–64]. A shift in all Raman bands to lower range of frequency is often observed particularly in the measurements that performed under ambient conditions [54]. It appears that an increase in alumina component in the SiO_2–xAl_2O_3 supports could stabilize the surface rhenium species as the first type of isolated monomeric ReO_4^- tetrahedra metathesis active structure whereas the proportion of the second type decreased. The intensity of Raman bands also increased with increasing amount of surface rhenium oxides as determined by the ICP-OES results. The Re/Si50Al catalyst that exhibited the highest propylene yield and good catalyst stability had the highest proportion of isolated monomeric ReO_4^- tetrahedral with relatively strong bond strength.

4 Conclusions

The role of silica–alumina composition in the unconventional metathesis of ethylene and 2-pentene has been investigated over the Re_2O_7/SiO_2–Al_2O_3 catalysts at 35 °C, GHSV 3,000 h^{-1}, and ethylene/2-pentene mole ratio 3. The SiO_2–Al_2O_3 composition has strong influence on the acidity, the metal–support interaction, and the dispersion of Re-active species. Higher amount of Re metal remained on the catalysts was observed in the Al_2O_3 rich Re_2O_7/SiO_2–xAl_2O_3 catalysts ($x \geq 50$ wt% Al_2O_3), corresponding to the stronger metal–support interaction. These characters also suggest a well dispersion of Re-active species as a monolayer of the isolated ReO_4^- species. The second type of the isolated monomeric ReO_4^- tetrahedral structure with a weaker Re–O-support bond appeared in all the catalysts except the one supported on pure alumina. The optimum amount of alumina in the SiO_2–Al_2O_3 was determined to be 50 wt% Al_2O_3 in which the highest propylene yield was obtained. The isomerization of the initial 1-butene product into 2-butenes and a subsequent secondary metathesis reaction between these 2-butenes and excess ethylene enhanced the propylene yield over the Re_2O_7/SiO_2–Al_2O_3 catalysts.

Acknowledgments The financial supports from the Thailand Research Fund (TRF), the Office of Higher Education Commission (CHE), and the CU-NRU (AM1088A) are gratefully acknowledged. The authors would like to thank the Royal Golden Jubilee Ph.D. scholarship from TRF and SCG chemicals Co., Ltd for W.P.

References

1. Mol JC (2004) J Mol Catal A Chem 213:39
2. Mol JC (1999) Catal Today 51:289
3. Luckner RC, Wills GB (1973) J Catal 28:83
4. Ivin KJ, Mol JC (1997) Olefin metathesis and metathesis polymerization. Academic Press, San Diego
5. Park YK, Lee CW, Kang NY, Choi WC, Choi S, Oh SH, Park DS (2010) Catal Surv Asia 14:75
6. Cornil B, Herrmann AW, Schogl R, Wong C (2000) A concise encyclopedia catalysis from A to Z. Wiley, New York
7. Gartside RJ, Stanley SJ (2011) C_5 metathesis for increased propylene, In: AIChE ethylene producers conference proceedings
8. Phongsawat W, Netivorruksa B, Suriye K, Dokjampa S, Praserthdam P, Panpranot J (2012) J Nat Gas Chem 21:83
9. Phongsawat W, Netivorruksa B, Suriye K, Dokjampa S, Praserthdam P, Panpranot J (2012) J Nat Gas Chem 21:158
10. Cosyns J, Chodorge J, Commereuc D, Torck B (1998) Hydrocarbon Process 77:61
11. Sibeijn M, Mol JC (1990) Appl Catal 67:279
12. Moulijn JA, Mol JC (1988) J Mol Catal 46:1
13. Andreini A, Xiaoding X, Mol JC (1986) Appl Catal 27:31
14. Sibeijn M, Spronk R, van Veen JAR, Mol JC (1991) Catal Lett 8:201
15. Sheu FC, Hong CT, Hwang WL, Shih CJ, Wu JC, Yeh CT (1992) Catal Lett 14:297
16. Balcar H, Hamtil R, Zilkova N, Cejka J (2004) Catal Lett 97:25
17. Onaka M, Oikawa T (2002) Chem Lett 8: 850
18. Oikawa T, Ookoshi T, Tanaka T, Yamamoto T, Onaka M (2004) Microporous Mesoporous Mater 74:93
19. Balcar H, Cejka J (2002) Macromol Symp 293:43
20. Martin-Aranda RM, Cejka J (2010) Top Catal 53:141
21. Zukal A, Siklova H, Cejka J (2008) Langmuir 24:9837
22. Gommes CJ, Friedrich H, Wolters M, De Jongh PE, De Jong KP (2009) Chem Mater 21:1311
23. Schmidt F (2001) Appl Catal. A 221:15
24. Ellison A, Coverdale AK, Dearing PF (1983) Appl Catal 8:109
25. Kapteijn F (1980) Catalytic metathesis of unsaturated esters by alumina supported rhenium oxide. PhD thesis, Amsterdam
26. Xu X, Boelhouwer C, Vonk D, Benecke JI, Mol JC (1985) J Mol Catal 36:47
27. Xiaoding X, Boelhouwer C, Vonk D, Benecke JI, Mol JC (1986) J Mol Catal 36:47
28. Mandelli D, Van Vliet MCA, Arnold U, Sheldon RA, Schuchardt U (2001) J Mol Catal A Chem 168:165
29. Xiaoding X, Mol JC, Boelhouwer C (1986) J Chem Soc Faraday Trans 1F(82):2707
30. Bakala PC, Briot E, Millot Y, Piquemal JY, Bregeault JM (2008) J Catal 258:61
31. Andreini A, Mol JC (1985) J Chem Soc Faraday Trans 1F(81):1705
32. Bregeault J-M, El Ali B, Martin J, Martin C, Derdar F, Bugli G, Delamar M (1988) J Mol Catal 46:37

33. Debecker DP, Hauwaert D, Stoyanova M, Barkschat A, Rodemerck U, Gaigneaux EM (2010) Appl Catal. A 391:78
34. Aritani H, Fukuda O, Yamamoto T, Tanaka T, Imamura S (2000) Chem Lett 1:66
35. Handzlik J, Ogonowski J, Stoch J, Mikolajczyk M, Michorczyk P (2006) Appl Catal. A 312:213
36. Handzlik J, Ogonowski J, Stoch J, Mikolajczyk M (2005) Catal Lett 101:65
37. Mol JC (1994) Catal Lett 23:113
38. Debecker DP, Bouchmella K, Poleunis C, Eloy P, Bertrand P, Gaigneaux EM, Mutin PH (2009) Chem Mater 21:2817
39. Handzlik J, Sautet P (2008) J Catal 256:1
40. Mol JC, Andreini A (1988) J Mol Catal 46:151
41. Spronk R, Andreini A, Mol JC (1991) J Mol Catal 65:219
42. Rodella CB, Cavalcante JAM, Buffon R (2004) Appl Catal A 274:213
43. Rost AMJ, Schneider H, Zoller JP, Herrmann WA, Kuhn FE (2005) J Organomet Chem 690:4712
44. Okada K, Tomita T, Kameshima Y, Yasumori A, MacKenzie KJD (1999) J Mater Chem 9:1307
45. Amigues P, Chauvin Y, Commereuc D, Lai CC, Liu YH, Pan JM (1990) Hydrocarbon Process Int Ed 69:79
46. Kapteijn F, Homburg E, Mol JC (1983) J Chem Thermodyn 15:147
47. Chauvin Y, Commereuc D (1992) J Chem Soc Chem Commun 462
48. Handzlik J, Ogonowski J (1998) Politechnika Krakowska, seria Inzynieria i, eds. Technologia Chemiczna, Kraków
49. Wang Y, Chen Q, Yang W, Xie Z, Xu W, Huang D (2003) Appl Catal A 250:25
50. Wagner CD, Riggs WM, Davis LE, Moulder JF, Muilenberg GE (1979) Handbook of X-ray photoelectron spectroscopy. Perkin-Elmer Corporation, Eden Prairie
51. Balcar H, Zilkova N, Bastl Z, Dedecek J, Hamtil R, Brabec L, Zukal A, CŒejka J (2007) Stud Surf Sci Catal 170:1145
52. Yuan Y, Iwasawa Y (2002) J Phys Chem B 106:4441
53. Stoyanova M, Rodemerck U, Bentrup U, Dingerdissen U, Linke D, Mayer RW, Lansink Rotgerink HGJ, Tacke T (2008) Appl Catal A 340:242
54. Okal J, Baran J (2001) J Catal 203:466
55. Edreva-Kardjieva RM, Vuurman MA, Mol JC (1992) J Mol Catal 76:297
56. Daniell W, Weingand T, Knozinger H (2003) J Mol Catal A Chem 204–205:519
57. Lacheen HS, Cordeiro PJ, Iglesia E (2006) J Am Chem Soc 128:15082
58. Vuurman MA, Stufkens DJ, Oskam A, Wachs IE (1992) J Mol Catal 76:263
59. Olsthoorn AA, Boelhouwer C (1976) J Catal 44:207
60. Bregeault J-M (1992) Catalyse homogene par les complexes des metaux de transition. Masson, Paris
61. Wang L, Hall WK (1983) J Catal 82:177
62. Williams KPJ, Harrison K (1990) J Chem Soc Faraday Trans 86:1603
63. Wachs IE (1996) Catal Today 27:437
64. Okal J, Kepinski L, Krajczyk L, Drozd M (1999) J Catal 188:140